

## Diffusion in Minerals: An Overview of Published Experimental Diffusion Data

**John B. Brady**

*Department of Geosciences  
Smith College  
Northampton, Massachusetts 01063, U.S.A.  
jbrady@smith.edu*

**Daniele J. Cherniak**

*Department of Earth & Environmental Sciences  
Rensselaer Polytechnic Institute  
Troy, New York 12180, U.S.A.  
chernd@rpi.edu*

### INTRODUCTION

Although geologists have been thinking and writing about diffusion in minerals, magmas, and rocks since early in the 20<sup>th</sup> century (e.g., Penrose 1914; Van Orstrand 1915; Bowen 1921; Eskola 1934; Duffell 1937; Reynolds 1947; Garrels 1949), very few experimental measurements of diffusion in minerals by geologists were published until the 1960's. The development of commercial electron microprobes in the late 1960's made it possible to measure compositional zoning in minerals on a micron scale, which provided both the motivation for and a means of determining diffusion coefficients. This led to a significant increase in the rate of publication of papers on diffusion in minerals during the 1970's (see **Fig. 1**). Other technological advances (e.g., secondary ion mass spectrometry) have further increased interest in diffusion data, leading to a continued growth of published diffusion coefficients and to the application of a host of experimental designs and measurement techniques (e.g., vapor deposition, Rutherford backscattering, nuclear reactions) that have expanded the range of measurable diffusivities (see Watson and Baxter 2007, Fig. 5; Watson and Dohmen 2010; Cherniak et al. 2010).

As interest in diffusion and the number of published diffusion coefficients have grown, several compilations of diffusion data for minerals have been published to assist researchers in finding the data they need (Harrop 1968; Askill 1970; Freer 1980, 1981; Brady 1995). However, such reviews do not provide easy (electronic) access to the data and they become quickly dated in an active field. Therefore, we have assembled a database of published experimental diffusion data for minerals and have made it available on the internet (<http://diffusion.smith.edu>), both as a searchable dataset and as downloadable files in various formats. As of this writing, our dataset includes 484 diffusion coefficient entries extracted from 223 papers. It is a work in progress. We know that the database is incomplete and, like any compilation, that it may contain mistakes, misinterpretations, and omissions. We hope that those who publish diffusion data and/or use the database will help us correct, improve, and extend it. This chapter presents some of the insights we have gained from examining the assembled data, which may serve as a context for the more detailed comparisons and evaluations of diffusion data in this RiMG volume.

Published sources for the diffusion data in the database are all included in the references for this chapter. A look at the minerals represented in the database gives a snapshot in time

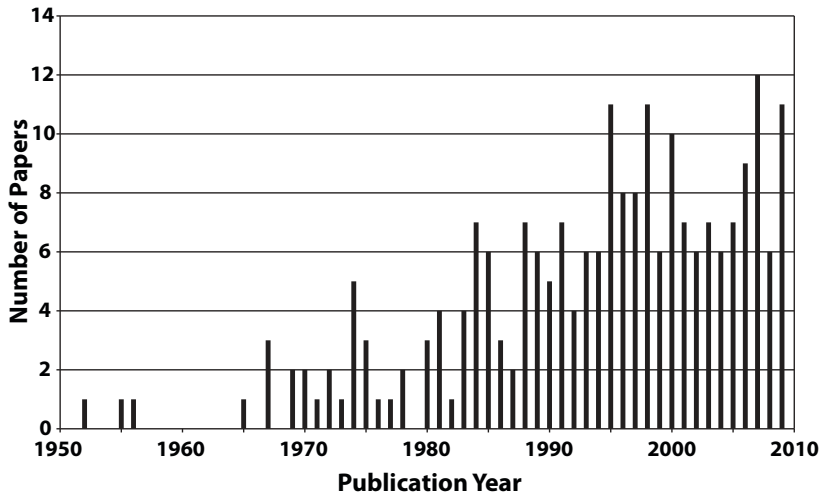


**Figure 1.** Numbers of published papers in the mineral diffusion database are shown here by date of publication on a bar graph. There were very few publications of experimentally determined diffusion coefficients for minerals until the 1970's, but there has been significant growth in the publication rate of diffusion papers since then.

of the research interests of the kinetics community. Over 75% of the diffusion coefficients are for silicates, with the most attention given to feldspars (16%), followed by pyroxenes (14%), olivine (12%), and garnet (8%) (see Fig. 2A). Of the silicates, data for micas (3%) and amphiboles (1.6%) are in short supply relative to the mineral abundance. Of the non-silicates, phosphates (apatite and monazite) are first (8%), followed by oxides (6%), carbonates (4%), and sulfides (3%). Many minerals have not been studied. Most of the measurements are of tracer diffusion coefficients (49%) or self-diffusion coefficients (40%), with only 11% interdiffusion coefficients, although some of the self-diffusion coefficients were calculated from interdiffusion experiments. Data for tracer diffusion or self-diffusion of 45 elements are included. The greatest number of measurements was made on oxygen diffusion (14%). Also numerous are data for Sr (8%), Ca (6%), Mg (6%), Pb (5%), H (4%), Si (4%), and Ar (4%) (see Fig. 2B).

### ARRHENIUS RELATIONS

Following the suggestion of Arrhenius (1889) and others, most papers in the database (93%) provide a linear fit to their diffusion data on a  $\log_{10}D$  vs.  $1/T$  diagram, reporting the slope of the fit as  $(E_a/R)$  and the intercept as  $\log_{10}D_0$ .  $E_a$  is the “activation energy”,  $R$  is the gas constant, and  $D_0$  is the diffusivity extrapolated to infinite temperature  $T$ . Linearity (or near linearity) is expected on Arrhenius diagrams for rate constants, such as diffusion coefficients, as long as the kinetic process uses the same mechanism over the range of temperatures studied (see Lasaga 1998, p. 60). For this reason, Arrhenius diagrams can be helpful not only in smoothing experimental data, but also in comparing diffusion coefficients among minerals, diffusing species, physical conditions, etc. The database enables users to make such comparisons easily.

An example of an Arrhenius comparison among minerals is given for oxygen diffusion in Figure 3. Figure 3A shows data for the self-diffusion of oxygen, typically  $^{18}\text{O}$ , in a variety of minerals in the presence of water or water vapor. Figure 3B shows data for the self-diffusion of oxygen in minerals under nominally anhydrous conditions. It is evident from the

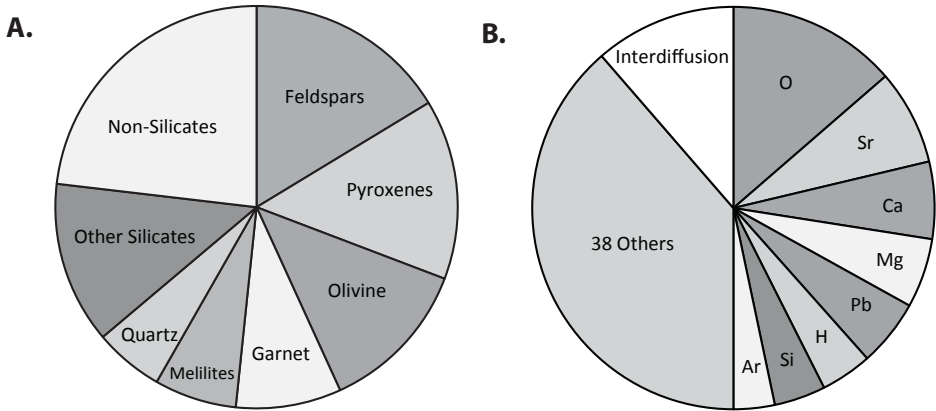


**Figure 2.** Percentages of diffusion data for the 484 entries in the database identified in terms of host mineral (A.) and of diffusing element (B.) are shown on pie charts. The key for each graph gives the pie shades clockwise, starting at the top.

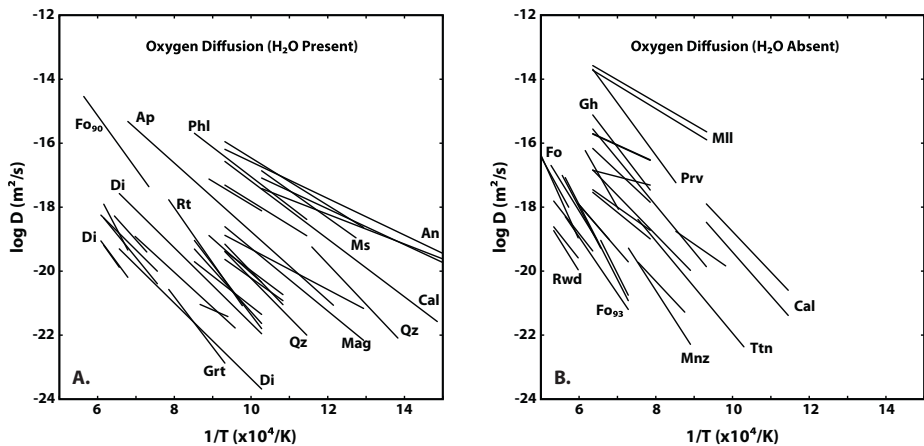


**Figure 3.** Arrhenius lines for oxygen diffusion in minerals in the presence of water or water vapor (A.) and under anhydrous conditions (B.). In A., lines for anorthite (An), muscovite (Ms), calcite (Cal), quartz (Qz), diopside (Di), garnet (Grt), rutile (Rt), olivine (Fo90), apatite (Ap), and phlogopite (Phl) are labeled. In B., lines for melilite (Mll), perovskite (Prv), calcite (Cal), titanite (Ttn), monazite (Mnz), olivine (Fo93), ringwoodite (Rwd), forsterite (Fo), and gehlenite (Gh). The two lines with the low slopes are nepheline and leucite. In general, the activation energy (slope) is higher for diffusion under anhydrous conditions. See Zheng and Fu (1998) for further information on oxygen diffusion under hydrous and anhydrous conditions.

diagrams that, on average, the activation energy for oxygen diffusion in the presence of water is lower (average = 214 kJ/mol) than for “dry” diffusion of oxygen (average = 278 kJ/mol). For minerals that have been studied under both hydrous and anhydrous conditions, diffusion coefficients for the dry experiments are smaller. These features have been interpreted by many workers to mean that the diffusing species is different (e.g.,  $\text{OH}^{-1}$  or  $\text{H}_2\text{O}$ ) when water is present (e.g., Yund and Anderson 1974). A quantitative model of the role of oxygen speciation during diffusion (such as  $\text{H}_2\text{O}$  during  $^{18}\text{O}$  diffusion) can be found in Zhang et al. (1991).

There are too many lines to label them all at the scale of Figure 3, but several minerals have been labeled on each diagram. There is a general trend for minerals with more open structures

to have higher oxygen self-diffusion coefficients, although there are obvious exceptions (e.g., rutile vs. diopside). This trend observed for diffusion of oxygen is at best a rule of thumb and can be misleading because factors other than space in the crystal structure affect diffusivities (see Moore et al. 1998, for a discussion of O diffusion in rutile). Nevertheless, similar relations are observed for the diffusion of other elements. Ranges of diffusivity versus inverse temperature from the diffusion database for nearly all studied elements are shown in **Figure 4** for several common mineral groups. As is the case for oxygen, diffusion coefficients for different minerals have restricted, if overlapping, ranges. In compiling Figure 4, diffusion coefficients for noble gases (He, Ar) and small cations (H, Li) have been omitted to display more clearly ranges that reflect the bulk of the diffusion data. Attempts to use these relations to predict diffusion coefficients quantitatively have had modest success (e.g., Zheng and Fu 1998; Fortier and Giletti 1989; Zhao and Zheng 2007) and will be discussed later in this review.

Arrhenius comparisons for diffusion of different elements in one mineral can be found throughout this volume. As an example, an Arrhenius diagram for all database entries for quartz is given here as **Figure 5**. For diffusion of cations in quartz, diffusion coefficients for more highly charged cations are generally lower (at the same temperature) than for cations of lower charge. Similarly, activation energies for diffusion of more highly charged cations are generally higher. As a rule of thumb with many exceptions, these trends apply to all the data in the diffusion database as shown in **Figure 6**. Almost all of the anion diffusion data in the database are for oxygen. Oxygen (-2) diffusivities for dry experiments (Fig. 3B), occupy the same range of values as +2 cations in Figure 6, suggesting that charge, whether positive or negative, has a similar inhibiting effect on diffusion that is proportional to the absolute value of the charge.

The influence of the size of an atom on its diffusion coefficient also can be seen in Figure 5 for quartz by looking at the data for the elements Li, Na, and K, which have the same charge but different sizes. This effect is also displayed nicely for alkali elements by albite and orthoclase

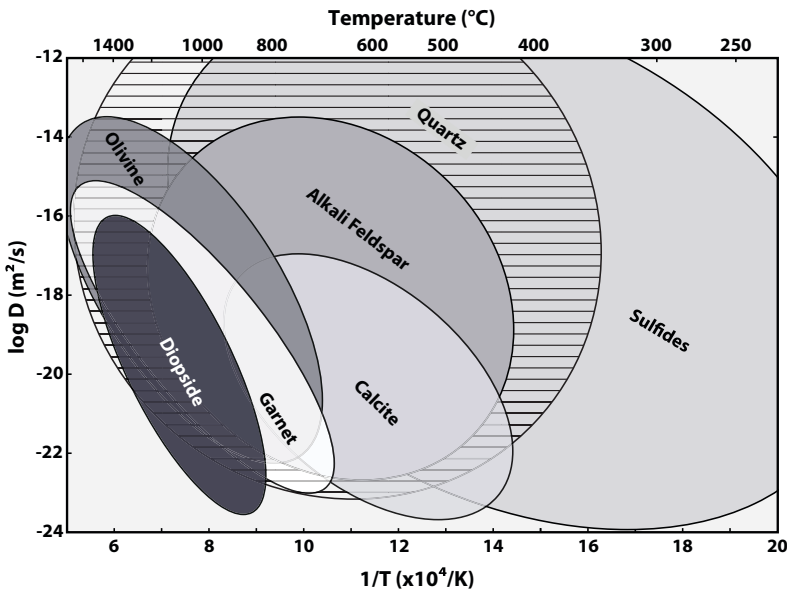


**Figure 4.** Schematic Arrhenius diagram showing the approximate ranges of measured diffusion coefficients and temperatures for all elements (except H, He, Ar, and Li) in several common minerals or mineral groups in the diffusion database.

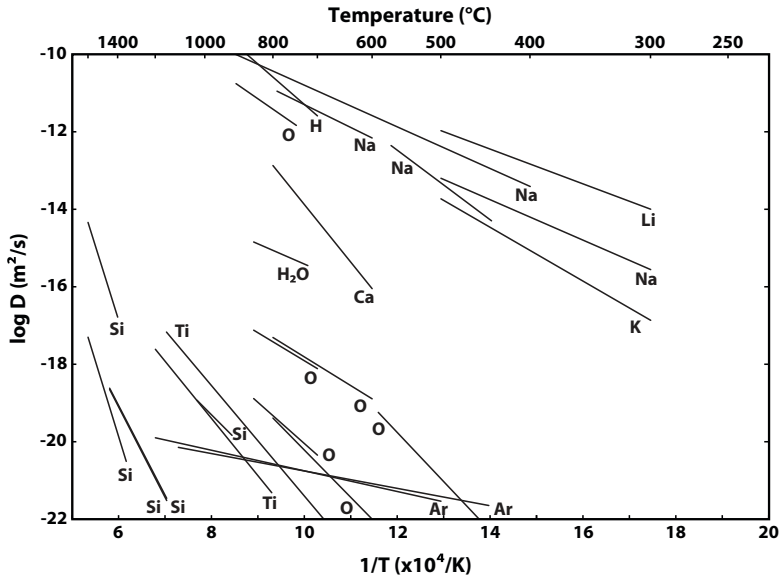


**Figure 5.** Arrhenius lines for diffusion in quartz for all entries in the database under nominally dry conditions. For cations, diffusion coefficients are generally lower and activation energies are generally higher for more highly charged cations in quartz. Interestingly, oxygen (-2) occupies the same range of diffusivities as +2 cations. Noble gases, such as Ar, follow other trends (see Baxter 2010).

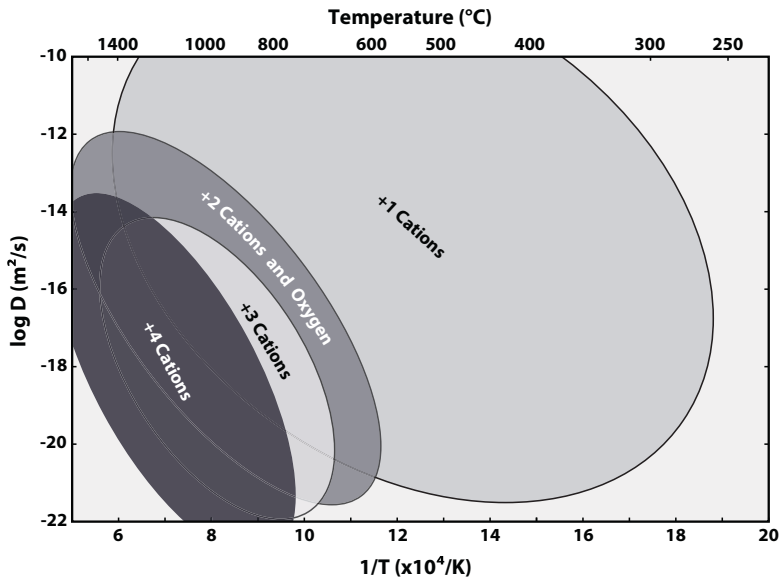


**Figure 6.** Schematic Arrhenius diagram showing the ranges of measured diffusion coefficients and temperatures for diffusing cations of different charge in the diffusion database. There is considerable overlap of the fields, but for the same temperature more highly charged cations are likely to have a smaller diffusion coefficient. Similarly, as a generalization with many exceptions, diffusion of more highly charged cations is likely to have a larger activation energy. Oxygen (-2) diffusion coefficients under dry conditions (Fig. 3B) occupy the same range as +2 cations.

(see Gilletti and Shanahan 1997; Cherniak 2010, Fig. 7). However, it is difficult to find good examples of this relationship for diffusion of +2 or +3 cations in minerals in the database, perhaps because the relative differences in size are smaller. Database data for diffusion of +3 REE in diopside and zircon and for +2 cations in some feldspar compositions also exhibit this effect.

A problem with showing diffusion data on Arrhenius diagrams is that the uncertainties in measurements tend to be forgotten when the data are represented by a straight thin line. Data for the tracer diffusion of alkali atoms in albite, mentioned in the previous paragraph, are shown in **Figure 7** in a way that emphasizes the effect on Arrhenius diagrams of uncertainties in activation energy ( $E_a$ ) and  $\log_{10}D_0$ . In Figure 7, several lines are drawn for the diffusion of each element. The middle line (solid) uses the reported  $E_a$  and  $\log_{10}D_0$ . The two dashed lines use the reported  $E_a$  and  $\log_{10}D_0$ , but adds to or subtracts from those values their reported uncertainties. The original diffusion data are shown along with curved solid lines that bound a two-sigma 95% confidence interval, which is slightly narrower in the center of the interval. A band of uniform width is drawn about the center line to show a simplified range of possible diffusion coefficients for each temperature that might be used if only the reported uncertainties in  $E_a$  and  $\log_{10}D_0$  are available. Users of the database should be careful not to overestimate the accuracy of diffusion measurements.

## DIFFUSION COMPENSATION DIAGRAMS

Another way to show interesting relationships among sets of diffusion data is to examine the compensation, or Meyer-Neldel, effect. The “compensation effect” refers to a positive linear

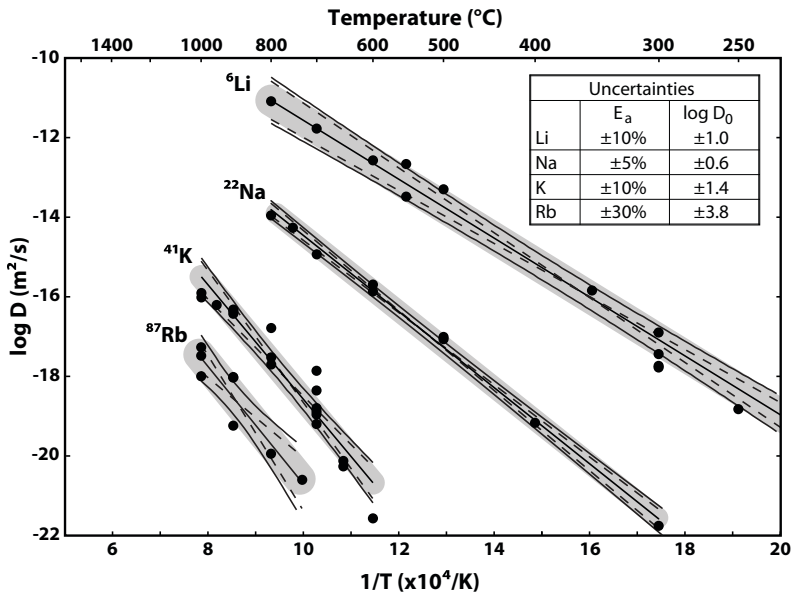


**Figure 7.** Data and Arrhenius lines for diffusion of Li, K, and Rb in albite from Gilletti and Shanahan (1997) and for diffusion of Na in albite from Kasper (1975). The Arrhenius lines are bounded by curved, 95% confidence-interval boundaries. Dashed lines are calculated by using two-sigma uncertainties in the activation energy (slope) and  $\log D_0$  (intercept), pairing the largest  $E_a$  with the largest  $\log D_0$  and the smallest  $E_a$  with the smallest  $\log D_0$ . The shaded bands give the uncertainty uniformly over the experimental temperature range, based on the widest separation of the dashed lines.

correlation between the activation energy for diffusion ( $E_a$ ) and the log of the pre-exponential factor ( $D_0$ ) for diffusion of various elements within a particular material, or diffusion of a particular ionic or molecular species within a range of materials. The dependence has the form

$$E_a = \mathbf{a} + \mathbf{b} \log(D_0)$$

where the factors  $\mathbf{a}$  and  $\mathbf{b}$  are specific to a particular material, diffusion mechanism, or diffusing species. While perhaps inadequate for accurate predictive purposes, compensation relationships do provide general insight into the ways in which crystal character influences diffusion and help identify anomalies where different diffusion mechanisms may apply.

There has been continued examination of the phenomenon of diffusion compensation and explanations in the literature of the compensation (Meyer-Neldel) law through molecular dynamic models (e.g., Boisvert et al. 1995) and statistical mechanics (e.g., Roginskii and Khait 1960; Yelon and Movaghar 1990; Yelon et al. 1992; Almond and West 1986, 1987). Essentially, compensation can be considered the result of a quasi-linear dependence of the activation energy for diffusion on the activation entropy (e.g., Winchell 1969). Materials and/or species with large activation barriers for diffusion compensate for the difficulty in surmounting these barriers by increasing the frequency of their attempts to diffuse (e.g., Boisvert et al. 1995).

Reasonable conformance to diffusion compensation trends has been observed for glasses (e.g., Winchell 1969; Hoffman 1980). Compensation was first considered with respect to diffusion in minerals in Hart's (1981) study, followed by Sneeringer et al. (1984) who considered Sr and Sm diffusion in diopside. Bejina and Jaoul (1997) later explored these relations for Si diffusion in silicates, and more recently the compilation of Zhao and Zheng (2007) examined diffusion compensation for a range of mineral phases and diffusants.

Plots of compensation relations are shown for a variety of diffusants (Figs. 8-10) and mineral phases (Figs. 11-12) from the database. Statistically good correlations are found for Mg (Fig. 8A), Pb (Fig. 8B), rare-earth elements (REE, Fig. 9A), and Si (Fig. 9B). Not shown, but similarly good compensation relations are observed for Sr and Ca, and for the alkaline earth elements as a group. Data for the alkali elements Na and K show less good correlations, in part due to the limited range of activation energies observed. Oxygen diffusion data show a broad compensation trend ( $R^2 = 0.58$ ) across minerals that is slightly improved ( $R^2 = 0.71$ ) if only the dry experiments are considered (see also Zheng and Fu 1998). The few He data in the database show a good compensation line. Ar data show a good line only for the hydrous silicates (Zhao and Zheng 2007), with most anhydrous silicate data well off this trend. Uncertainties in the reported data should be shown on compensation diagrams, where differences among results are clearly displayed. For many elements, there are not enough measured diffusivities in minerals to yield a statistically meaningful compensation relation. Data selection can change the resulting compensation line and should be done with consideration, for example, of the types of experimental and analytical techniques used to determine diffusion coefficients and the limitations in each case, as well as the potential for measured diffusivities to be affected by non-diffusional processes.

All of the data we used to create the compensation diagrams are for tracer diffusion or self-diffusion. In most cases, interdiffusion data are not available in sufficient numbers to give meaningful compensation diagrams. One possible exception is Fe-Mg interdiffusion for which we have 15 measurements in minerals, which are shown in Figure 10. The data for Fe-Mg interdiffusion data plot near to the compensation line for Mg, but the Fe-Mg interdiffusion compensation line has a much different slope and intercept and an  $r^2$  value of only 0.36. Many factors make interdiffusion more complex than self-diffusion or tracer diffusion, typically including a strong dependence on composition that may include a "thermodynamic factor" (Brady 1975) and be especially sensitive to  $f_{O_2}$  or  $f_{H_2O}$ .

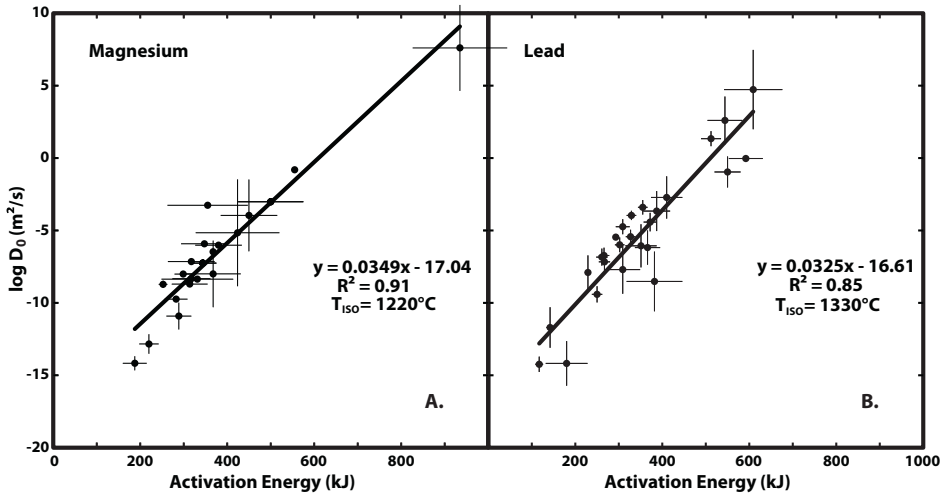


**Figure 8.** Compensation diagrams for the diffusion of Mg (A.) and Pb (B.) in all minerals in the database. Uncertainties for activation energy and  $\log D_0$  are shown if they were reported in the original paper. Equations for the compensation lines and isokinetic temperatures ( $T_{\text{iso}}$ ) are shown.

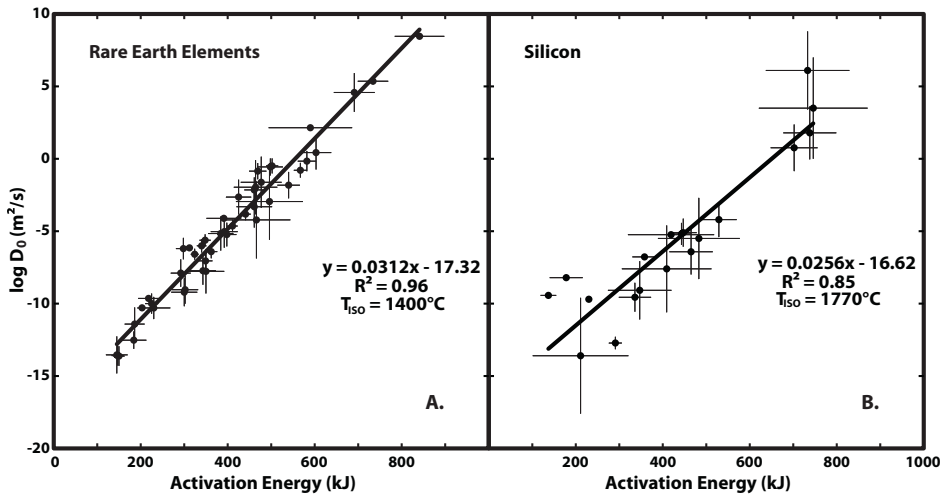


**Figure 9.** Compensation diagrams for the diffusion of REE (A.) and Si (B.) in all minerals reported in the database (except fluorite for REE). Uncertainties for activation energy and  $\log D_0$  are shown if they were reported in the original paper. Equations for the compensation lines and isokinetic temperatures ( $T_{\text{iso}}$ ) are shown.

For diffusion following a compensation relation, there will be a critical temperature (sometimes called the “isokinetic” or “crossover” temperature) at which diffusion of all species in a particular mineral (or in all minerals for a particular diffusing species) will be the same. The physical significance of these temperatures is generally not well understood, but they may have practical importance when considering relative diffusivities of specific elements in a mineral phase over a range of geologically relevant temperatures if the “crossover” point is within the temperature range of interest. The isokinetic temperature ( $T_{\text{iso}}$ ) is inversely related



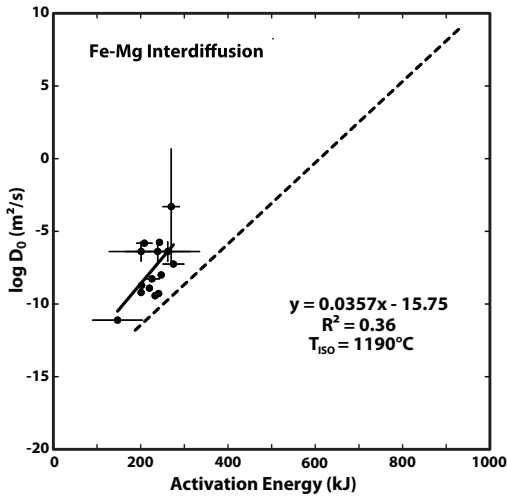
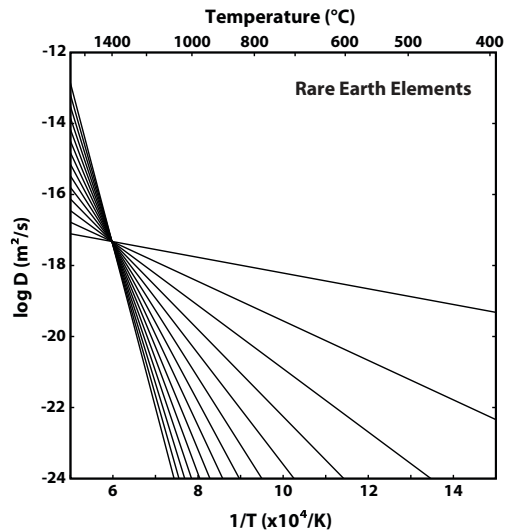


**Figure 10.** Compensation diagram for Fe-Mg interdiffusion in the minerals olivine, orthopyroxene, periclasite, and spinel. Shown for comparison is the compensation line for Mg diffusion from Figure 8a.

**Figure 11.** Pattern of Arrhenius lines for diffusion of rare earth elements (REE) in all minerals in the database (except fluorite) that would be observed if all diffusion coefficients followed exactly the compensation law fit to the REE diffusion data in Figure 9A. All Arrhenius lines pass through the same  $D$  ( $4.8 \times 10^{-18} \text{ m}^2/\text{s}$ ) at the isokinetic temperature of 1400 °C. Compare this diagram to the observed Arrhenius lines in Figure 12B that have been extrapolated to the edge of the diagram.



to the slope ( $S$ ) of the compensation line following the relation:

$$T_{\text{ISO}}(\text{K}) = \frac{1}{S \times R}$$

where  $R$  is the gas constant (e.g., Winchell 1969; Lasaga 1998, p.81). For the compensation diagrams in this paper, the expression used is:

$$T_{\text{ISO}}(\text{°C}) = \frac{1000}{S \times 8.314 \times 2.303} - 273.15$$

The constant 1000 is needed because  $E_a$  is in kJ/mol, and the constant 2.303 is needed because base 10 logarithms were used. An example of “ideal” Arrhenius relations for diffusion of rare-earth elements (REE), based on the compensation relation from Figure 9A, is shown

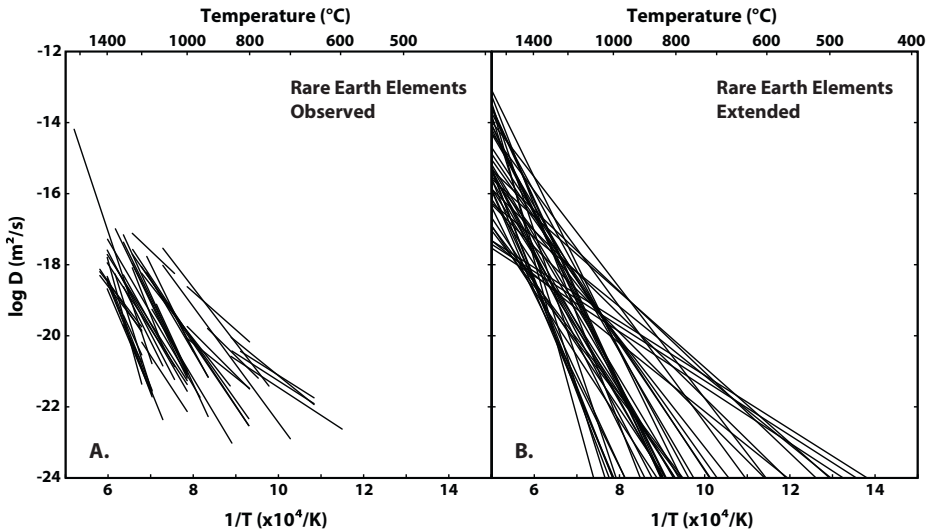


**Figure 12.** (A.) Arrhenius lines for diffusion of rare earth elements (La, Nd, Sm, Eu, Dy, Er, Yb) as reported for all minerals in the database (except fluorite). (B.) The same Arrhenius lines as in A., but with each Arrhenius line extended beyond its measurement region to the boundaries of the diagram to show the lines intersecting. Compare this diagram with ideal diffusion compensated lines in Figure 11.

in Figure 11. All Arrhenius lines pass through  $T_{ISO}$ , which is 1400 °C, and have the  $\log D$  value of  $-17.32$ . For comparison, an Arrhenius diagram for the observed REE diffusivities is shown in Figure 12A. The Arrhenius lines of Figure 11A have been extended in Figure 12B to show the range of actual intersections and to give a sense of the uncertainties that accompany even very good compensation lines.

Different groups of elements show systematically different compensation relations. One interesting observation from the compensation lines for various elements is a trend of increasing slope of the compensation lines with decreasing charge among divalent, trivalent, and tetravalent cations (see **Fig. 13**). This trend may reflect the greater options for jumps for less-highly charged

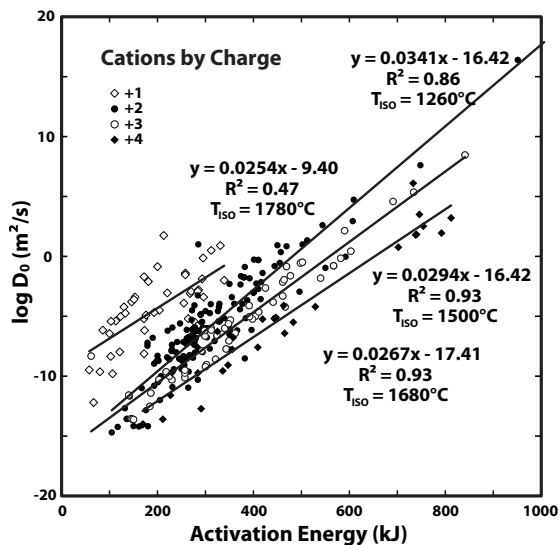


**Figure 13.** Compensation diagram for the diffusion of cations arranged by charge in all oxygen-based minerals in the database (no sulfides, halides, etc.). The positions of the data points change systematically as charge increases from +1 to +4. The slopes of the compensation lines increase as charge increases from +2 to +4, although the slope of the +1 compensation line does not follow the trend.

cations, effects due to charge-balance requirements, or differences in diffusion mechanisms between respective groups of cations. Univalent cations seem to depart from this trend (see Fig. 13), but there is considerable scatter in the data and a limited range of activation energies for these diffusants.

Data for diffusion of a variety of elements in a specific mineral, rather than diffusion of one element in many minerals, also can show good correlations for diffusion compensation. However, because of variations in compensation relations with charge (Fig. 13), the mineral data are generally fit more closely by a line if the diffusants are similar in charge. Examples of compensation relations from the database are shown for the minerals calcite and quartz in **Figure 14** and for diopside and plagioclase in **Figure 15**. Calcite (Fig. 14A) diffusion data for constituent elements C, Ca, and O along with Mg, Sr, Pb, Dy, La, Nd are closely modeled by a compensation line. Quartz (Fig. 14B) exhibits two compensation trends, one for univalent and divalent cations (Li, Na, K, Ca), and another for more highly charged cations (Si, Ti), which as above show a steeper slope than for the less highly-charged species. Data for oxygen diffusion in quartz are spread over the two cation trends. Diopside (Fig. 15A) exhibits very good compensation relations for diffusion of all measured elements (Al, Ca, Ce, Dy, Fe, La, Mg, Nd, O, Pb, Si, Sm, Sr, Th, U) except H, He and Li. Plagioclase data (Fig. 15B) are less well correlated, but the fit is improved considerably if the +1 cations (K, Li, Na) and the +4 cation (Si) are omitted, leaving Ca, O, Mg, Nd, Pb, Rb, and Sr.

Several other minerals show good compensation relations only if some diffusing elements are ignored. Zircon data for Dy, Hf, O, Pb, Si, Sm, Th, Ti, U, and Yb, are fit well ( $R^2 = 0.90$ ) if the He data are omitted. Olivine data are not fit well unless only the +2 diffusants (Ca, Co, Mg, Mn, Ni) are considered ( $R^2 = 0.85$ ), and has a better fit ( $R^2 = 0.89$ ) if the +2 interdiffusion data are added. Fluorite data for Ca, Dy, Nd, Sr, Y, Yb are correlated ( $R^2 = 0.91$ ) if the F data are removed. Fluorapatite data for Ca, Dy, La, Mn, Nd, O, P, Pb, Sm, Sr, and Yb are correlated ( $R^2 = 0.90$ ) if He, F, and U data are removed. Based on these observations, it

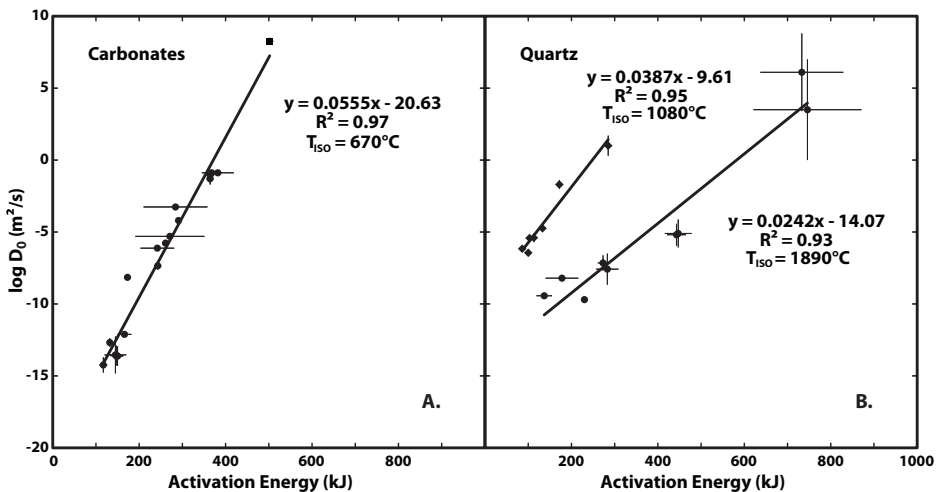


**Figure 14.** Compensation diagram for diffusion of many different elements in carbonate minerals (A.) and quartz (B.). Uncertainties for activation energy and  $\log D_0$  are shown if they were reported in the original paper. For carbonates, all data are for calcite except for one (square) point for diffusion of C in dolomite. For quartz, the data points fit by the upper line are for Li, Na, K, and Ca. The data points fit by the lower line are for Si and Ti. Not shown are data points for O, which fall on or between the other lines and show no apparent trend.

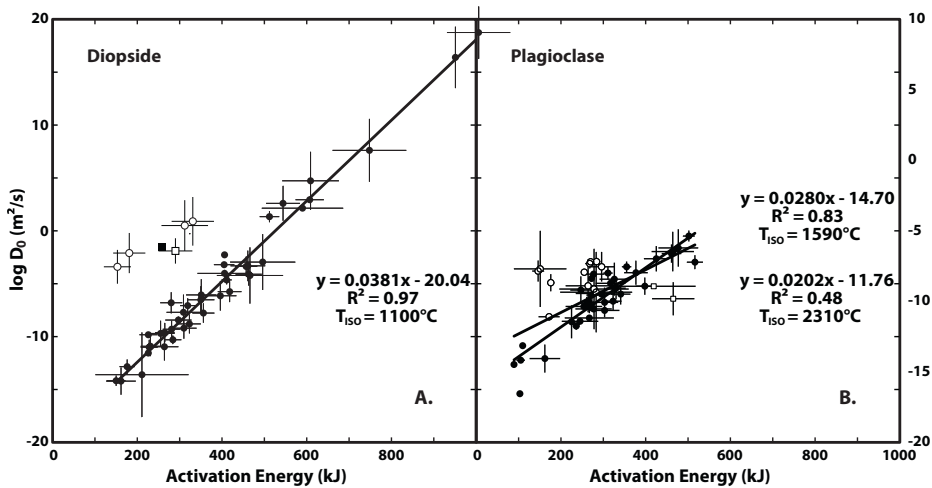


**Figure 15.** Compensation diagram for diffusion of many elements in diopside (A.) and plagioclase (B.). Uncertainties for activation energy and  $\log D_0$  are shown if they were reported in the original paper. For diopside, the compensation line shown is fit to all elements except H (open circles), He (open square), and Li (solid square). The linear fit to the data is very good if the H, He, and Li values are not included. For plagioclase, the compensation line fit has a steeper slope and is improved considerably if the +1 cations (Li, Na, K, Rb - open circles) and the +4 cation (Si - open squares) are omitted.

appears that charge and size of the diffusing species may be as important as the host mineral in determining diffusivity. Despite these seemingly good agreements in specific cases, there are other minerals, such as alkali feldspar ( $R^2 = 0.62$ , **Fig. 16**), that conform less well to linear diffusion compensation trends. While this departure may in part be a consequence of large uncertainties in extant diffusion data and/or experimental artifacts contributing to erroneous Arrhenius relations, it may in some cases reflect the complexity of substitutional processes, diffusional mechanisms, effects of material composition, or other factors influencing diffusion. Similarly, while reasonably good correlations are found for diffusion of divalent cations, the

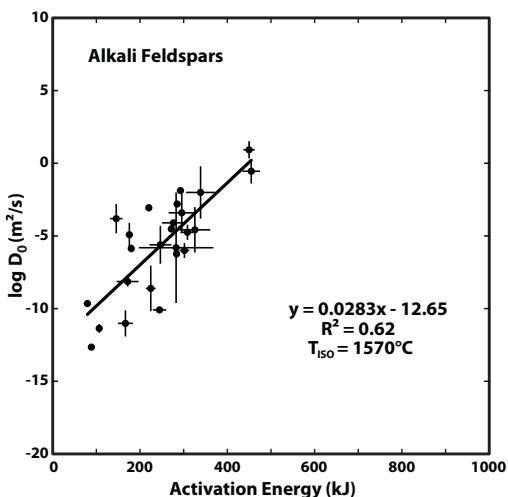


**Figure 16.** Compensation diagram for diffusion of Ar, Ba, Ca, K, Li, Na, O, Pb, Sr in alkali feldspars (albite, adularia, microcline, orthoclase, sanidine). There is considerable scatter in the data, although the fit of the compensation line can be improved by selecting the diffusing species by charge.

(trivalent) rare-earth elements, and silicon in a range of mineral types, there are nonetheless significant outliers, and other elements (including univalent elements as noted above) that have considerably poorer correlations.

Compilation, establishment, and interpretation of diffusion compensation relations face two distinct difficulties: (1) the selective exclusion of data that are perceived as “outliers” without strong justification for their exclusion, and (2) the inclusion of diffusion data that may be compromised by non-diffusional processes or experimental artifacts that render Arrhenius relations non-descriptive of volume diffusion. For these reasons, the use of compensation lines to predict diffusion coefficients is likely to be at best a rough approximation. However, the use of compensation relations to help identify “outliers” or “unusual,” and therefore suspect (or very interesting!), diffusion data is quite reasonable.

### IONIC POROSITY

Similarities in diffusion data for ions of similar size and charge, such as those discussed in this review, have led a number of authors to examine relationships among diffusion coefficients and the “open space” or “ionic porosity” of minerals (e.g., Dowty 1980; Fortier and Giletti 1989; Dahl 1996; Zheng and Fu 1998; Zhao and Zheng 2007). These studies are based on the concept that mobility of ions will be enhanced by more “open space” available in a mineral’s structure. Crystal structure data and ionic size are then used to understand and to predict diffusion data. Most authors have used the ionic radii of Shannon (1976) to calculate ionic porosity, using either anion volume alone (anion porosity) or the volume of all ions (total ionic porosity). Both diffusivity and activation energy may be sensitive to ionic porosity, because a more closely packed structure should raise the potential energy barrier to diffusion.

With the large compilation of diffusion data in our database, it is possible to explore diffusion-porosity trends for a variety of minerals. In general, we found only weak dependence of both diffusivity and activation energy on ionic porosity. The best correlations were observed for oxygen, which makes sense because oxygen is a large diffusing species that may have more difficulty moving through a dense structure than would a small cation. Data for oxygen diffusion under dry conditions (cf. Fig 3B) for all studies in the database are shown in **Figure 17**. In Figure 17A, diffusivities at 1000 °C are shown to increase with increasing anion porosity. However, the trend is a broad one with little quantitative prediction value. In Figure 17B, activation energy for oxygen diffusion in the same minerals decreases with increasing anion porosity. Although the trend line in Figure 17B is statistically more meaningful, the scatter of the data is still quite large and make the trend of only limited use for quantitative prediction. Similar graphs of rare earth element (REE) diffusion data from the database are given as **Figure 18**. These are the same data that defined a good compensation relationship in Figure 9A. It is apparent from Figure 18 that ionic porosity is not a good predictor of either diffusivity at 1000 °C or activation energy for diffusion of REE. Data for the diffusion of many other elements yielded similarly unimpressive correlations with ionic porosity. Although several authors have been encouraged by the predictive value of ionic porosity (e.g., Fortier and Giletti 1989; Dahl 1996; Zheng and Fu 1998; Zhao and Zheng 2007), the trends we observed from the database diffusivities are only approximate. Whether they are useful for quantitative prediction depends on the accuracy needed from the prediction. Zhao and Zheng (2007) improve their  $\log D$  vs. porosity trend lines by adjusting the ionic porosity with temperature. Perhaps more precise diffusion data, restricted by lab or measurement technique, and corrected for temperature and other factors, such as anisotropy, will improve the quantitative utility of a porosity approach.

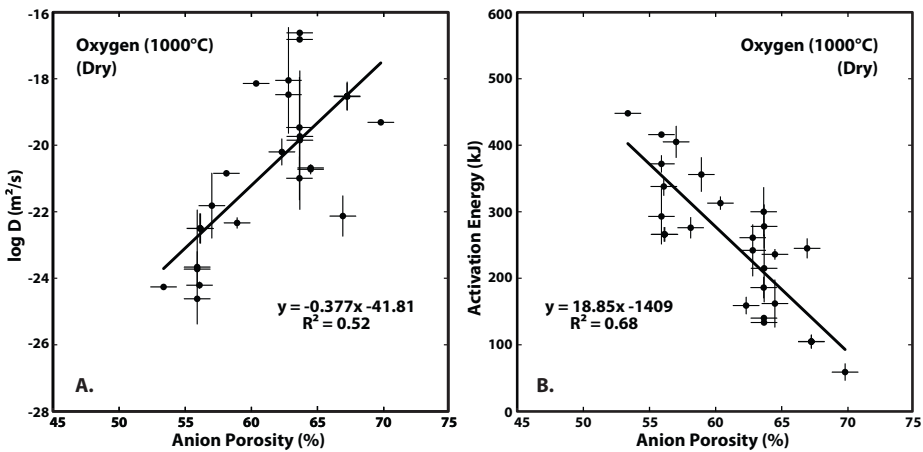


**Figure 17.** (A.) Variation of diffusivity at 1000 °C with anion porosity for oxygen diffusion under dry condition for all minerals in the database. (B.) Variation of activation energy with anion porosity for oxygen diffusion under dry condition for all minerals in the database. Anion porosity data are mostly from Zhao and Zheng (2007), supplemented with data from Shannon (1976) and unit cell data from the Am Mineral crystal structure database (MSA 2010). Uncertainties for activation energy and  $D$  are shown if uncertainties were reported in the original paper. Uncertainties for porosity are shown as  $\pm 1\%$ . Diffusivity increases and activation energy decreases with increased anion porosity, although there is considerable scatter in the data.

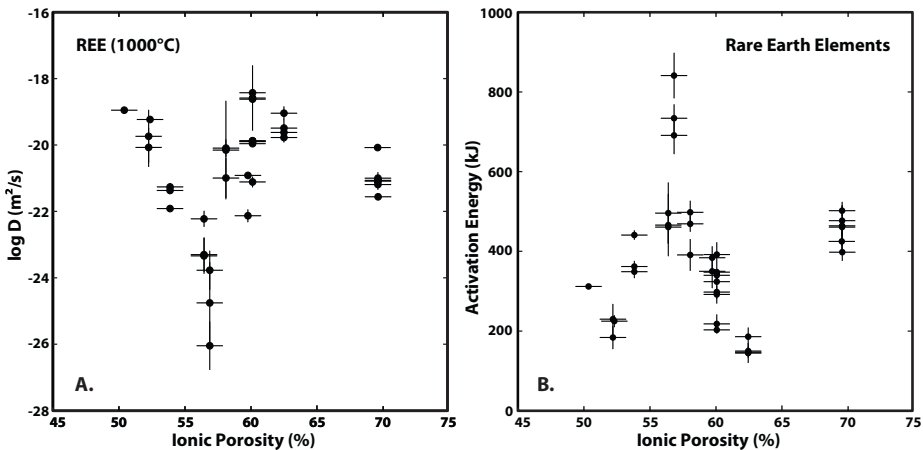


**Figure 18.** (A.) Variation of diffusivity at 1000 °C with ionic porosity for rare earth element (REE) diffusion for all minerals in the database. (B.) Variation of activation energy with ionic porosity for REE diffusion for all minerals in the database. Ionic porosity data are mostly from Zhao and Zheng (2007), supplemented with data from Shannon (1976) and unit cell data from the Am Mineral crystal structure database (MSA 2010). Uncertainties for activation energy and  $\log D$  are shown if uncertainties were reported in the original paper. Uncertainties for porosity are shown as  $\pm 1\%$ . The scatter in the data is too large to obtain a statistically significant trend.

## DIFFUSION ANISOTROPY

Diffusion in a non-isometric crystal may vary with the transport direction. Two or three diffusion coefficients (depending on crystal symmetry), along principal directions, are needed to describe fully diffusion in such anisotropic minerals. The principal directions are along crystallographic axes for tetragonal, trigonal, hexagonal, and orthorhombic crystals, but are less predictably oriented for monoclinic and triclinic crystals (see Nye 1985, Chapter XI; Zhang 2010). Many experimentalists report diffusivities for only one direction in their samples. However, 79 diffusivities in 56 papers in the database were measured in two or three directions. Of these, no anisotropy in diffusivity was observed in 39 cases, whereas some anisotropy was observed in 39 cases.

Measurements that revealed no diffusion anisotropy are listed in **Table 1**. Because uncertainties in diffusion measurements can be significant, reader should remember that the lack of observed anisotropy is only as certain as the diffusivities themselves. Measurements that did exhibit diffusion anisotropy are listed in **Table 2**. Also shown in Table 2 are values for the maximum observed difference in  $\log D$  for the temperatures studied and the difference in activation energy expressed as a fraction of the smallest activation energy. For comparison, these differences are shown in **Figures 19 and 20** as histogram plots. As can be seen in Figure 19, most differences of diffusivity with direction are less than an order of magnitude. Eight have differences greater than one order of magnitude.

Interestingly, many of the measurements with significant anisotropy are for diffusion of oxygen, which suggests that diffusion direction matters more for larger diffusing species. This is consistent with the concept of ionic porosity as a control on diffusivity, as discussed in the previous section. If ionic porosity varies with direction, then diffusion in the direction with the greatest directional porosity should be fastest. Directional porosity is more difficult to evaluate quantitatively than total ionic porosity because a model is needed to rate constrictions versus average open space. We do not believe that the existing diffusion data warrant analysis in such detail. However, we have examined qualitatively the structures of the minerals for which anisotropic diffusivities are reported, looking for obvious open paths or channels in “space filling” representations. In every case, measured diffusion of oxygen is fastest in the direction with more apparent directional porosity (e.g., parallel to the c-axis of quartz or diopside, or parallel to the structural sheets in micas). In most but not all cases, diffusion of other elements also is fastest in the direction with more apparent directional porosity.

Differences in activation energies for minerals with diffusion anisotropy are shown for comparison in Figure 20. Differences have been normalized by the magnitude of the activation energy to show a fractional value. For many of the measurements, the observed activation energies are quite similar, and most are within a factor of two. It is curious that activation energies can be so similar in a mineral, while diffusivities and the pre-exponential factor can vary by an order of magnitude or more. An example is He diffusion in zircon (Cherniak et al. 2009). This relationship makes sense when considering migration of small noble gas atoms that are not charged and may move interstitially. The pre-exponential factor is related to crystal structure, jump frequency and distance, while the activation energy is related to defect formation energy and the energy required to form an activated complex. Things may be more complex for diffusion of charged species, those that may migrate on a range of different lattice sites (or those restricted to only certain lattice sites because of their size), those requiring charge compensation, and those that may migrate by differing mechanisms depending on, for example,  $f_{\text{O}_2}$  conditions, the presence of water or other hydrous species. We can see no overall trend in the anisotropy of activation energies, although several of the largest differences once again are for oxygen diffusion.

**Table 1.** Diffusion measurements that revealed no diffusion anisotropy.

Mineral	Mineral Composition	Diffusing Species	Citation
albite	Ab <sub>98</sub>	Sr	Giletti and Casserly (1994)
anorthite	An <sub>96</sub>	Sr	Giletti and Casserly (1994)
apatite	syn. and natural	Mn	Cherniak (2005)
apatite	Durango	Sr	Cherniak and Ryerson (1993)
apatite	natural	U	Cherniak (2005)
calcite		Ca	Farver and Yund (1996)
calcite		<sup>18</sup> O	Farver (1994)
corundum		Ar	Thomas et al. (2008)
diopside	0.4-2.4%Fe	<sup>44</sup> Ca	Dimanov et al. (1996)
diopside	2% Fe	<sup>44</sup> Ca	Dimanov and Jaoul (1998)
diopside	synthetic	<sup>26</sup> Mg	Pacaud (1999)
diopside	3.6% Fe	<sup>26</sup> Mg	Pacaud (1999)
fluorapatite		He	Cherniak et al. (2009)
fluorapatite		Pb	Watson et al. (1985)
fluorapatite		Sm	Watson et al. (1985)
fluorapatite		Sr	Watson et al. (1985)
hornblende		Sr	Brabander and Giletti (1995)
labradorite	An <sub>62</sub>	<sup>22</sup> Na	Behrens et al. (1990)
labradorite	Ab <sub>36</sub>	Sr	Giletti and Casserly (1994)
mullite	2(Al <sub>2</sub> O <sub>3</sub> )SiO <sub>2</sub>	<sup>18</sup> O	Fielitz et al. (2001)
olivine	Fo <sub>100</sub> and Fo <sub>90</sub>	Ar	Thomas et al. (2008)
olivine	Fo <sub>90</sub>	H	Demouchy and Mackwell (2006)
olivine	Fo <sub>90</sub>	<sup>18</sup> O	Costa and Chakraborty (2008)
olivine	Fo <sub>100</sub>	<sup>18</sup> O	Jaoul et al. (1983)
olivine	Fo <sub>89</sub>	O	Houlier et al. (1988)
olivine	Fo <sub>90</sub> Fa <sub>10</sub>	<sup>30</sup> Si	Houlier et al. (1990)
olivine	Fo <sub>90</sub>	<sup>29</sup> Si	Costa and Chakraborty (2008)
olivine	Fo <sub>89</sub>	<sup>30</sup> Si	Houlier et al. (1988)
orthopyroxene	En <sub>100</sub>	Ar	Thomas et al. (2008)
orthopyroxene	En <sub>99.8</sub> Fs <sub>0.02</sub>	Eu	Cherniak and Liang (2007)
orthopyroxene	En <sub>100</sub> -syn.	H	Stalder and Skogby (2003)
quartz		Ar	Thomas et al. (2008)
quartz		Ti	Cherniak et al. (2007b)
sphalerite	Zn <sub>.98</sub> Fe <sub>.02</sub> S	Zn↔Fe	Mizuta (1988)
titanite		O	Morishita et al. (1996)
titanite		Sr	Cherniak (1995b)
tremolite		Sr	Brabander and Giletti (1995)
zircon		<sup>30</sup> Si	Cherniak (2008)
zircon		O	Watson and Cherniak (1997)



**Table 2.** Diffusion measurements that revealed diffusion anisotropy.

Mineral	Mineral Composition	Diffusing Species	log <i>D</i> Difference Max	<i>E<sub>a</sub></i> Diff Fraction	Citation
albite	Ab <sub>98,5</sub>	Li	0.30	0.00	Giletti & Shanahan (1997)
anorthite	An <sub>95</sub>	<sup>25</sup> Mg	0.48	0.09	LaTourette & Wasserburg (1998)
anorthite	An <sub>95</sub>	<sup>44</sup> Ca	0.17	0.13	LaTourette & Wasserburg (1998)
anorthite	An <sub>95,6</sub>	Li	0.20	0.00	Giletti & Shanahan (1997)
anorthoclase	Or <sub>27</sub>	Sr	0.66	0.00	Cherniak & Watson (1992)
calcite		<sup>13</sup> C	0.25	0.00	Kronenberg et al. (1984)
diopside	essentially pure	<sup>18</sup> O	1.73	0.00	Farver (1989)
diopside	1.8% Fe	<sup>26</sup> Mg	0.42	0.54	Zhang et al. (2009)
diopside		H	1.00	0.00	Woods et al. (2000)
diopside	syn., Fe-free	O	0.94	0.42	Ingrin et al. (2001)
diopside	Di <sub>95</sub>	Pb	0.11	0.06	Cherniak (1998)
fluorapatite		F,Cl↔OH	3.43	0.25	Brenan (1993)
gehlenite	syn.	<sup>18</sup> O	2.42	0.61	Yurimoto et al. (1989)
gehlenite		K	0.40	0.03	Ito & Ganguly (2004)
labradorite	An <sub>62</sub>	<sup>22</sup> Na	0.66	0.05	Behrens et al. (1990)
labradorite	An <sub>67</sub>	Ba	0.23	0.06	Cherniak (2002)
monazite		Pb	0.70	0.00	Smith & Giletti (1997)
oligoclase	An <sub>23</sub>	Ba	0.70	0.24	Cherniak (2002)
oligoclase	An <sub>23</sub>	Pb	1.36	0.36	Cherniak (1995a)
olivine	Fo <sub>83</sub> to Fo <sub>92</sub>	<sup>42</sup> Ca	0.39	0.07	Coogan et al. (2005)
olivine	Fo <sub>91</sub>	Cr	0.83	0.18	Ito & Ganguly (2006)
olivine	Fo <sub>90</sub>	H	0.88	0.26	Demouchy & Mackwell (2006)
olivine	Fo <sub>90</sub>	Ni	0.78	0.00	Petry et al. (2004)
olivine	Fo <sub>100</sub> syn.	Mg	0.78	0.00	Chakraborty et al. (1994)
olivine	Fo <sub>100</sub> syn.	H <sub>2</sub> O	1.12	0.10	Demouchy & Mackwell (2003)
orthoclase	Or <sub>93</sub>	Pb	0.97	0.02	Cherniak (1995a)
orthopyroxene	En <sub>96</sub>	Cr	0.70	0.00	Ganguly et al. (2007)
orthopyroxene	En <sub>88</sub> Fs <sub>12</sub>	Mg	0.58	0.36	Schwandt et al. (1998)
pyrrhotite	Fe <sub>0,9</sub> S	<sup>55</sup> Fe	0.25	0.00	Condit et al. (1974)
quartz	SiO <sub>2</sub>	<sup>18</sup> O	2.23	0.47	Dennis (1984)
quartz	SiO <sub>2</sub>	<sup>18</sup> O	3.11	0.65	Giletti & Yund (1984)
quartz	natural	Si	0.06	0.01	Cherniak (2003)
rutile	natural and syn.	Hf	0.38	0.34	Cherniak et al. (2007a)
titanite		Nd	0.45	0.20	Cherniak (1995b)
tourmaline	elbaite	H↔D	0.87	0.59	Desbois & Ingrin (2007)
zircon		He	1.75	0.01	Cherniak et al. (2009)

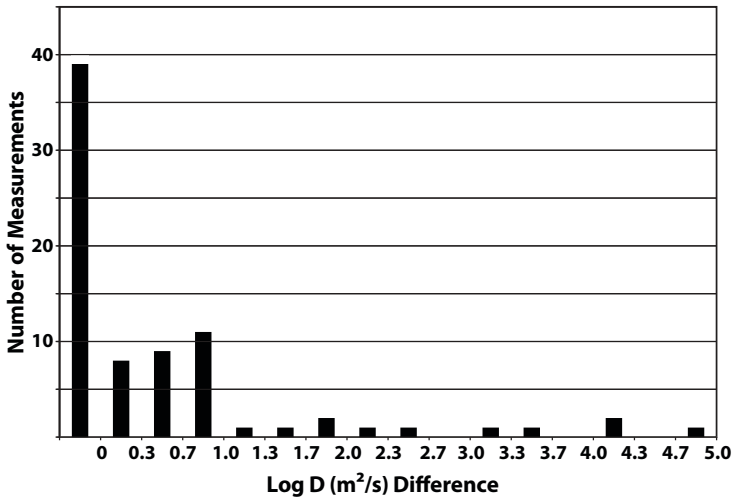


**Figure 19.** Histogram of measured diffusivities in the mineral diffusion database for which diffusion anisotropy has been determined (see Table 2). Numbers of measurements are grouped in bins (numbers shown bound the bins) according to the maximum observed difference in  $\log D$  for the temperatures studied. Thirty-nine measurements reported no anisotropy. Thirty-nine measurements found anisotropy. The three largest anisotropy values are for micas, reported by Fortier and Giletti (1991).

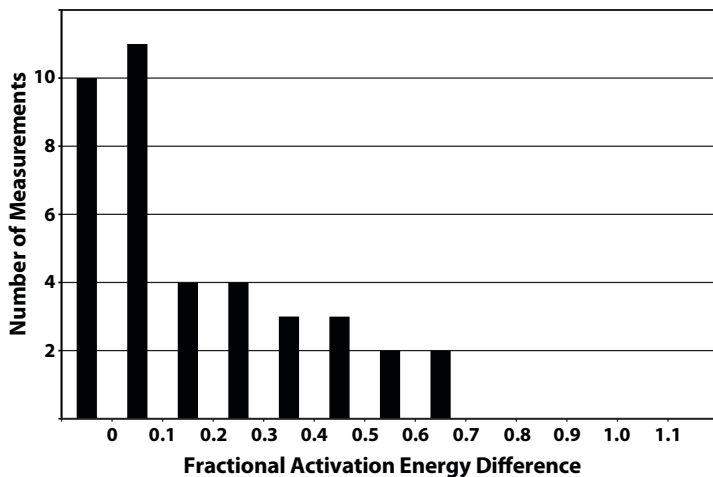


**Figure 20.** Histogram of measured diffusivities in the mineral diffusion database for which diffusion anisotropy has been determined (see Table 2). Numbers of measurements are grouped in bins (numbers shown bound the bins) according to the difference in observed activation energy expressed as a fraction of the smaller reported activation energy. Activation energies for diffusion in different directions in anisotropic minerals are within a factor of two for most samples.

## CONCLUDING REMARKS

The accomplishments of the geoscience community in measuring and interpreting diffusion data for minerals over the last four decades are quite impressive. Our database now contains diffusion data for 45 elements and over 40 mineral groups, some with many different compositions represented. With these data available in electronic format, it is possible to look for empirical relationships and to test models against measured diffusivities. In this review we have highlighted some of the general trends concerning diffusion in minerals that can be demonstrated with the database. The keywords here are “general” and “trends.” Precise measurements of diffusion coefficients are experimentally difficult and most papers report data that have significant associated uncertainties. Collections of these data can improve the statistics of any interpretation, although differences among techniques and laboratories may cancel the theoretical gains.

Many opportunities exist to conduct experiments that will further our understanding of diffusion in minerals. We expect to see diffusion data for more minerals, more high pressure studies, more studies of the variation of diffusivities with mineral composition, and more interdiffusion experiments. Significant advances will come as we find ways to reduce the uncertainties inherent in diffusion measurements. Better characterization and understanding of the samples being studied will also help. We hope to see further development of dynamic models of transition states that can be combined with diffusion experiments to make good predictions that match and extend our measurements. We look forward to these advances and to the new data that you, our readers, will provide. Please help us keep the diffusion database up to date by sending us your data to post.

## ACKNOWLEDGMENTS

The authors wish to thank reviewers Y.-F. Zheng and Y. Zhang for their thoughtful comments and suggestions on drafts of this chapter.

## REFERENCES

- Almond DP, West AR (1986) Entropy effects in ionic conductivity. *Solid State Ionics* 18-19:1105-1109
- Almond DP, West AR (1987) The activation entropy for transport in ionic conductors. *Solid State Ionics* 23:27-35
- Arrhenius S (1889) On the reaction velocity of the inversion of cane sugar by acids. *Z Phys Chem* 4:226
- Askill J (1970) *Tracer Diffusion Data for Metals, Alloys, and Simple Oxides*. Plenum Press, New York
- Baxter EF (2010) *Diffusion of Noble Gases in Minerals*. *Reviews in Mineralogy & Geochemistry* 72:xxx-xxx
- Behrens H, Johannes W, Schmalzried H (1990) On the mechanisms of cation diffusion processes in ternary feldspars. *Phys Chem Miner* 17:62-78
- Bejjina F, Jaoul O (1997) Silicon diffusion in silicate minerals. *Earth Planet Sci Lett* 153:229-238
- Boisvert G, Lewis LJ, Yelon A (1995) Many-body nature of the Meyer-Neldel compensation law for diffusion. *Phys Rev Lett* 75:469-472
- Bowen NL (1921) Diffusion in silicate melts. *J Geol* 29:295-317
- Brabander DJ, Giletti BJ (1995) Strontium diffusion kinetics in amphiboles and significance to thermal history determination. *Geochim Cosmochim Acta* 59:2223-2238
- Brady JB (1975) Reference frames and diffusion coefficients. *Am J Sci* 275:954-983
- Brady JB (1995) Diffusion data for silicate minerals, glasses, and liquids: *In: Mineral Physics and Crystallography: A Handbook of Physical Constants*. Ahrens TH (ed) AGU Reference Shelf 2, American Geophysical Union, Washington, DC, p 269-290
- Brenan J (1993) Kinetics of fluorine, chlorine and hydroxyl exchange in fluorapatite. *Chem Geol* 110:195-210.
- Chakraborty S, Farver JR, Yund RA, Rubie DC (1994) Mg tracer diffusion in synthetic forsterite and San Carlos Olivine as a function of P, T and  $f_{O_2}$ . *Phys Chem Miner* 21:489-500
- Cherniak DJ (1995a) Diffusion of lead in plagioclase and K-feldspar; an investigation using Rutherford backscattering and resonant nuclear reaction analysis. *Contrib Mineral Petrol* 120:358-371

- Cherniak DJ (1995b) Sr and Nd diffusion in titanite. *Chem Geol* 125:219-232
- Cherniak DJ (1998) Pb diffusion in clinopyroxene. *Chem Geol* 150:105-117
- Cherniak DJ (2002) Ba diffusion in feldspar. *Geochim Cosmochim Acta* 66:1641-1650
- Cherniak DJ (2003) Silicon self-diffusion in single-crystal natural quartz and feldspar. *Earth Planet Sci Lett* 214:655-668
- Cherniak DJ (2005) Uranium and manganese diffusion in apatite. *Chem Geol* 219:297-308
- Cherniak DJ (2008) Si diffusion in zircon. *Phys Chem Miner* 35:179-187
- Cherniak DJ (2010) Diffusion in feldspars. *Reviews in Mineralogy & Geochemistry* 72:xxx-xxx
- Cherniak DJ, Hervig R, Koepke J, Zhang Y, Zhao D (2010) Analytical methods in diffusion studies. *Reviews in Mineralogy & Geochemistry* 72:xxx-xxx
- Cherniak DJ, Liang Y (2007) Rare earth element diffusion in natural enstatite. *Geochim Cosmochim Acta* 71:1324-1340
- Cherniak DJ, Manchester J, Watson EB (2007a) Zr and Hf diffusion in rutile. *Earth Planet Sci Lett* 261:267-279
- Cherniak DJ, Ryerson FJ (1993) A study of strontium diffusion in apatite using Rutherford backscattering spectroscopy and ion implantation. *Geochim Cosmochim Acta* 57:4653-4662
- Cherniak DJ, Watson EB (1992) A study of strontium diffusion in K-feldspar, Na-K feldspar and anorthite using Rutherford backscattering spectroscopy. *Earth Planet Sci Lett* 113:411-425
- Cherniak DJ, Watson EB, Thomas JB (2009) Diffusion of helium in zircon and apatite. *Chem Geol* 268:155-166
- Cherniak DJ, Watson EB, Wark DA (2007b) Ti diffusion in quartz. *Chem Geol* 236:65-74
- Condit RH, Hobbs RR, Birchenall CE (1974) Self-diffusion of iron and sulfur in ferrous sulfide. *Oxid Met* 8:409-455
- Coogan LA, Hain A, Stahl S, Chakraborty S (2005) Experimental determination of the diffusion coefficient for calcium in olivine between 900 degrees C and 1500 degrees C. *Geochim Cosmochim Acta* 69:3683-3694
- Costa F, Chakraborty S (2008) The effect of water on Si and O diffusion rates in olivine and implications for transport properties and processes in the upper mantle. *Phys Earth Planet Inter* 166:11-29
- Dahl PS (1996) The effects of composition on retentivity of argon and oxygen in hornblende and related amphiboles: A field-tested empirical model. *Geochim Cosmochim Acta* 60:3687-3700
- Demouchy S, Mackwell SJ (2003) Water diffusion in synthetic iron-free forsterite. *Phys Chem Miner* 30:486-494
- Demouchy S, Mackwell SJ (2006) Mechanisms of hydrogen incorporation and diffusion in iron-bearing olivine. *Phys Chem Miner* 33:347-355
- Dennis PF (1984) Oxygen self-diffusion in quartz under hydrothermal conditions. *J Geophys Res* 89:4047-4057
- Desbois G, Ingrin J (2007) Anisotropy of hydrogen diffusion in tourmaline. *Geochim Cosmochim Acta* 71:5233-5243
- Dimanov A, Jaoul O (1998) Calcium self-diffusion in diopside at high temperature; implications for transport properties. *Phys Chem Miner* 26:116-127
- Dimanov A, Jaoul O, Sautter V (1996) Calcium self-diffusion in natural diopside single crystals. *Geochim Cosmochim Acta* 60:4095-4106
- Dowty E (1980) Crystal-chemical factors affecting the mobility of ions in minerals. *Am Mineral* 65:174-182
- Duffell S (1937) Diffusion and its relation to ore deposition. *Economic Geology* 32:494-510
- Eskola P (1934) A note on diffusion and reactions in solids. *Bulletin De La Commission Geologique De Finlande* 104:145-156
- Farver JR (1994) Oxygen self-diffusion in calcite; dependence on temperature and water fugacity. *Earth Planet Sci Lett* 121:575-587
- Farver JR, Yund RA (1989) Oxygen self-diffusion in diopside with application to cooling rate determinations. *Earth Planet Sci Lett* 92:386-396
- Farver JR, Yund RA (1996) Volume and grain boundary diffusion of calcium in natural and hot-pressed calcite aggregates. *Contrib Mineral Petrol* 123:77-91
- Fielitz P, Borchardt G, Schmücker M, Schneider H, Wiedenbeck M, Rhede D, Weber S, Scherrer S (2001) Secondary ion mass spectrometry study of oxygen-18 tracer diffusion in 2/1-mullite single crystals. *J Am Ceram Soc* 84:2845-2848
- Fortier SM, Gilotti BJ (1989) An empirical model for predicting diffusion coefficients in silicate minerals. *Science* 245:1481-1484
- Fortier SM, Gilotti BJ (1991) Volume self-diffusion of oxygen in biotite, muscovite, and phlogopite micas. *Geochim Cosmochim Acta* 55: 1319-1330.
- Freer R (1980) Self-diffusion and impurity diffusion in oxides. *J Mater Sci* 15:803-824
- Freer R (1981) Diffusion in silicate minerals and glasses: a data digest and guide to the literature. *Contrib Mineral Petrol* 76:440-454

- Ganguly J, Ito M, Zhang X (2007) Cr diffusion in orthopyroxene; experimental determination,  $^{53}\text{Mn}$ - $^{53}\text{Cr}$  thermochronology, and planetary applications. *Geochim Cosmochim Acta* 71:3915-3925
- Garrels RM (1949) Diffusion of ions through intergranular spaces in water-saturated rocks. *Geol Soc Am Bull* 60:1809-1828
- Giletti BJ, Casserly JED (1994) Strontium diffusion kinetics in plagioclase feldspars. *Geochim Cosmochim Acta* 58:3785-3793
- Giletti BJ, Shanahan TM (1997) Alkali diffusion in plagioclase feldspar. *Chem Geol* 139:3-20
- Giletti BJ, Yund RA (1984) Oxygen diffusion in quartz. *J Geophys Res* 89:4039-4046.
- Harrop PJ (1968) Self-diffusion in simple oxides (a bibliography). *J Mater Sci* 3:206-222
- Hart SR (1981) Diffusion compensation in natural silicates. *Geochim Cosmochim Acta* 45:279-291
- Hofmann AW (1980) Diffusion in natural silicate melts; a critical review. *In: Physics of Magmatic Processes*. Hargraves, RB (ed) Princeton University Press, p 385-418
- Houlier B, Cheraghmakani M, Jaoul O (1990) Silicon diffusion in San Carlos Olivine. *Phys Earth Planet Inter* 62:329-340
- Houlier B, Jaoul O, Abel F, Liebermann RC (1988) Oxygen and silicon self-diffusion in natural olivine at T = 1300 degrees C. *Phys Earth Planet Inter* 50:240-250
- Ingrin J, Pacaud L, Jaoul O (2001) Anisotropy of oxygen diffusion in diopside. *Earth Planet Sci Lett* 192:347-361
- Ito M, Ganguly J (2004) Potassium diffusion in melilite; experimental studies and constraints on the thermal history and size of planetesimals hosting CAIs. *Meteorit Planet Sci* 39:1911-1919
- Ito M, Ganguly J (2006) Diffusion kinetics of Cr in olivine and  $^{53}\text{Mn}$ / $^{53}\text{Cr}$  thermochronology of early solar system objects. *Geochim Cosmochim Acta* 70:799-809
- Jaoul O, Houlier B, Abel F (1983) Study of  $^{18}\text{O}$  diffusion in magnesium orthosilicate by nuclear microanalysis. *J Geophys Res* 88:613-624
- Kasper RB (1975) Cation and oxygen diffusion in albite. PhD Dissertation, Brown University, Providence, RI
- Kronenberg AK, Yund RA, Giletti BJ (1984) Carbon and oxygen diffusion in calcite; effects of Mn content and  $\text{P H}_2\text{O}$ . *Phys Chem Miner* 11:101-112
- Lasaga AC (1998) *Kinetic Theory in the Earth Sciences*. Princeton University Press, Princeton
- LaTourette T, Wasserburg GJ (1998) Mg diffusion in anorthite: implications for the formation of early solar system planetesimals. *Earth Planet Sci Lett* 158:91-108
- Mizuta T (1988) Interdiffusion rate of zinc and iron in natural sphalerite. *Econ Geol* 83:1205-1220
- Moore DK, Cherniak DJ, Watson EB (1998) Oxygen diffusion in rutile from 750 to 1000 degrees C and 0.1 to 1000 MPa. *Am Mineral* 83:700-711
- Morishita Y, Giletti BJ, Farver JR (1996) Volume self-diffusion of oxygen in titanite. *Geochem J* 30:71-79
- MSA (2010) The American Mineralogist crystal structure database. [http://www.minsocam.org/MSA/Crystal\\_Database.html](http://www.minsocam.org/MSA/Crystal_Database.html)
- Nye JF (1985) *Physical Properties of Crystals*. Oxford University Press, Oxford
- Pacaud L (1999) Mesure de l'autodiffusion de l'oxygène et du magnésium dans le diopside et applications. PhD Dissertation, Université de Paris 11, Orsay, France
- Penrose RAF Jr. (1914) Certain phases of superficial diffusion in ore deposits. *Econ Geol* 9:20-24
- Petry C, Chakraborty S, Palme H (2004) Experimental determination of Ni diffusion coefficients in olivine and their dependence on temperature, composition, oxygen fugacity, and crystallographic orientation. *Geochim Cosmochim Acta* 68:4179-4188
- Reich M, Ewing RC, Ehlers TA, Becker U (2007) Low temperature anisotropic diffusion of helium in zircon: implications for zircon (U-Th)/He thermochronometry. *Geochim Cosmochim Acta* 71:3119-3130 (NOT USED?)
- Reynolds DL (1947) The granite controversy. *Geol Mag* 84:209-223
- Roginskii SZ, Khait YuL (1960) The origin of the compensation effect in chemical kinetics. *Doklady Akademii Nauk SSSR* 130:366-369
- Schwandt CS, Cygan RT, Westrich HR (1998) Magnesium self-diffusion in orthoenstatite. *Contrib Mineral Petrol* 130:390-396
- Shannon RD (1976) Revised effective ionic radii and systematic studies of interatomic distances in halides and chalcogenides. *Acta Crystallogr* A32:751-767
- Smith HA, Giletti B (1997) Lead diffusion in monazite. *Geochim Cosmochim Acta* 61:1047-1055
- Sneeringer M, Hart SR, Shimizu N (1984) Strontium and samarium diffusion in diopside. *Geochim Cosmochim Acta* 48:1589-1608
- Stalder R, Skogby H (2003) Hydrogen diffusion in natural and synthetic orthopyroxene. *Phys Chem Miner* 30:12-19
- Thomas JB, Cherniak DJ, Watson EB (2008) Lattice diffusion and solubility of argon in forsterite, enstatite, quartz and corundum. *Chem Geol* 253:1-24

- Van Orstrand CE (1915) Preliminary report on the diffusion of solids. U.S. Geol Survey Professional Paper 95-G:83-96
- Watson EB, Baxter EF (2007) Diffusion in solid-Earth systems. *Earth Planet Sci Lett* 253:307-327
- Watson EB, Cherniak DJ (1997) Oxygen diffusion in zircon. *Earth Planet Sci Lett* 148:527-544
- Watson EB, Dohmen R (2010) Experimental methods in diffusion studies: *Reviews in Mineralogy & Geochemistry* 72:xxx-xxx
- Watson EB, Harrison TM, Ryerson FJ (1985) Diffusion of Sm, Sr, and Pb in fluorapatite. *Geochim Cosmochim Acta* 49:1813-1823
- Winchell P (1969) The compensation law for diffusion in silicates. *High Temp Sc* 1:200-215
- Woods SC, Mackwell SJ, Dyar MD (2000) Hydrogen in diopside; diffusion profiles. *Am Mineral* 85:480-487
- Yelon A, Movaghar B (1990) Microscopic explanation of the compensation (Meyer-Neldel) rule. *Phys Rev Lett* 65:618-620
- Yelon A, Movaghar B, Branz HM (1992) Origin and consequences of the compensation (Meyer-Neldel) law. *Phys Rev B (Condensed Matter)* 46:12244-12250
- Yund RA, Anderson TF (1974) Oxygen isotope exchange between potassium feldspar and KCL solution. *In: Geochemical Transport and Kinetics*. Hofmann AW, Giletti BJ, Yoder HS, Jr., and Yund RA (eds) Carnegie Institution of Washington, p 99-106
- Yurimoto H, Morioka M, Nagasawa H (1989) Diffusion in single crystals of melilite; I, Oxygen. *Geochim Cosmochim Acta* 53:2387-2394
- Zhang et al. (1991) MISSING
- Zhang X, Ganguly J, and Ito M (2009) Ca-Mg diffusion in diopside: tracer and chemical inter-diffusion coefficients. *Contrib Mineral Petrol* 159:175-186
- Zhang Y (2010) Diffusion in minerals and melts: theoretical background. *Reviews in Mineralogy & Geochemistry* 72:xxx-xxx
- Zhao Z-F, Zheng Y-F (2007) Diffusion compensation for argon, hydrogen, lead, and strontium in minerals: empirical relationships to crystal chemistry. *Am Mineral* 92:289-308
- Zheng Y-F, Fu B (1998) Estimation of oxygen diffusivity from anion porosity in minerals. *Geochem J* 32:71-89